2017

Coupled DEM-FEM analysis for simulating ballasted rail tracks

Ngoc Trung Ngo
University of Wollongong, trung@uow.edu.au

Buddhima Indraratna
University of Wollongong, indra@uow.edu.au

Cholachat Rujikiatkamjorn
University of Wollongong, cholacha@uow.edu.au

Coupled DEM-FEM analysis for simulating ballasted rail tracks

Abstract

Ballasted tracks play an essential role in its economy through transporting freight and bulk commodities between major cities and ports, and carrying passengers, particularly in urban areas. Ballast usually consists of hard and strong angular particles, which are derived from high strength unweathered rocks. Ballast aggregates undergo gradual and continuing degradation under cyclic train loadings. In this study, the load-deformation responses of ballasted rail tracks subjected to cyclic loading are studied experimentally using a large-scale Track Process Simulation Apparatus (TPSA), and numerically through a coupled discrete-continuum approach, namely, coupled DEM-FEM. Laboratory tests are carried out to examine the deformation and degradation responses of ballast subjected to cyclic train loading under a frequency of f=15 Hz and a lateral confinement of σxx=10 kPa. Test results reveal that significant settlements are observed during the initial load cycles, followed by gradually increased deformation, arriving at a steady value towards the end of testing. A rigorous coupling model based on discrete element method (DEM) and finite element method (FEM) is introduced to predict the load-deformation behaviour of the ballast assembly considering the interaction of discrete ballast grains and continuum subgrade. In this coupled model, the discrete ballast grains are modelled by DEM and the subgrade domain is modelled as a continuum by FEM. Interface elements are introduced to transmit the interacting forces and displacements between adjoining material domains (i.e. discrete and continuum) whereby the DEM transfers contact forces to the FEM, and then the FEM updates the displacements back to the DEM. The coupled model is validated by comparing the predicted ballast settlement responses with those obtained experimentally. Contact force distributions, stress contours and a corresponding number of broken bonds are analysed. This combined DEM-FEM model is also used to analyse the load-deformation of a fully instrumented track in Singleton, Australia, and the numerical predictions are compared with the field data.

Keywords

analysis, simulating, ballasted, rail, tracks, dem-fem, coupled

Disciplines

Engineering | Science and Technology Studies

Publication Details

Ngo, N., Indraratna, B. & Rujikiatkamjorn, C. (2017). Coupled DEM-FEM analysis for simulating ballasted rail tracks. 15th International Conference of the International Association for Computer Methods and Advances in Geomechanics (15th IACMAG) (pp. 1-12).

Coupled DEM-FEM analysis for simulating ballasted rail tracks

Ngoc Trung Ngo[a]*, Buddhima Indraratna[a], and Cholachat Rujikiatkamjorn[a]

[a]*Centre for Geomechanics and Railway Engineering, Faculty of Engineering and Information Sciences, University of Wollongong, Wollongong, NSW 2522, Australia; ARC Centre of Excellence for Geotechnical Science and Engineering, Australia*
**trung@uow.edu.au (Corresponding Author)*

Abstract

Ballasted tracks play an essential role in its economy through transporting freight and bulk commodities between major cities and ports, and carrying passengers, particularly in urban areas. Ballast usually consists of hard and strong angular particles, which are derived from high strength unweathered rocks. Ballast aggregates undergo gradual and continuing degradation under cyclic train loadings. In this study, the load-deformation responses of ballasted rail tracks subjected to cyclic loading are studied experimentally using a large-scale Track Process Simulation Apparatus (TPSA), and numerically through a coupled discrete-continuum approach, namely, coupled DEM-FEM. Laboratory tests are carried out to examine the deformation and degradation responses of ballast subjected to cyclic train loading under a frequency of f=15 Hz and a lateral confinement of σ_{xx}=10 kPa. Test results reveal that significant settlements are observed during the initial load cycles, followed by gradually increased deformation, arriving at a steady value towards the end of testing. A rigorous coupling model based on discrete element method (DEM) and finite element method (FEM) is introduced to predict the load-deformation behaviour of the ballast assembly considering the interaction of discrete ballast grains and continuum subgrade. In this coupled model, the discrete ballast grains are modelled by DEM and the subgrade domain is modelled as a continuum by FEM. Interface elements are introduced to transmit the interacting forces and displacements between adjoining material domains (i.e. discrete and continuum) whereby the DEM transfers contact forces to the FEM, and then the FEM updates the displacements back to the DEM. The coupled model is validated by comparing the predicted ballast settlement responses with those obtained experimentally. Contact force distributions, stress contours and a corresponding number of broken bonds are analysed. This combined DEM-FEM model is also used to analyse the load-deformation of a fully instrumented track in Singleton, Australia, and the numerical predictions are compared with the field data.

Keywords: Discrete Element Method, Interface Elements, Ballast, Rail Tracks

1. Introduction

Ground improvement techniques have been employed to improve road and railway embankment conditions and reclaimed lands in Australia. Ballasted rail tracks are the largest transportation infrastructure catering for public and freight transport in Australia. It is noted that rail embankments are usually subjected to large cyclic stresses due to heavier and faster trains inducing large deformations and degradation of the ballast layer [1, 2]. Ballast is an essential component of the rail track substructure, and it is commonly used for (i) distributing the wheel load from sleepers to the underlying subgrade, (ii) maintaining track alignment, and (iii) providing track drainage. It normally consists of medium to coarse gravel sized particles (10-53 mm) and a small proportion of sand size grains [3, 4]. Upon repeated train loading, ballast degrades to smaller sizes, which adversely decreases the shear strength and decreases the drainage capacity of the ballasted tracks [5-8].

Computational modelling approach has been widely applied to simulate granular materials, and various conventional continuum constitutive models have been introduced to capture their stress-strain behaviour of granular materials [9-11]. Considering the discrete nature of ballast particles, the continuum approach (e.g. Finite Element method–FEM) could not accurately capture their micromechanical behaviour mainly controlled by the fabric anisotropy, contact force distribution chains and strain

localization [12, 13]. Recently, the discrete element method (DEM) has been increasingly employed in the recent past as an alternative to the continuum-based methods for the study of granular materials. The DEM introduced by Cundall and Strack [14] has been increasingly adopted to study load-deformation behaviour of ballast aggregates [15-19], among others. The DEM enables deeper insight into the micromechanical characteristics of granular materials such as contact force distribution, fabric anisotropy, and particle breakage, that are almost impossible or unlikely to be measured in the laboratory [4, 20-24].

The use of DEM to model ballast under cyclic loads is required significantly computational extensive [3, 17, 25]. In these studies, the loading was limited to only a few hundred load cycles, and the role of angularity in view of varied shapes and sizes of grains could not be accurately simulated. Lu and McDowell [26] introduced a DEM model simulating ballast subjected to 100 load cycles and they presented that the proposed model could still obtain the correct stress-strain response of ballast. In this paper, a coupled DEM-FEM model was used to model an integrated and layered ballasted track. A ballast layer was modelled using the DEM, whereas sub-ballast and subgrade layers were modelled by the FEM. The interaction between ballast layer and subgrade was facilitated by a series of interface elements generated at the DEM and FEM boundary. The proposed model was validated by large-scale laboratory tests using Track Process Simulation Apparatus (TPSA).

2. Laboratory investigation

A large-scale Track Process Simulation Apparatus (TPSA) can accommodate a ballast specimen of: 800 mm × 600 mm × 600 mm was used to measure the deformation and degradation of ballast under cyclic loads [27], as shown Figure 1. Ballast was selected from Bombo quarry, New South Wales, Australia, then cleaned and sieved following to the Australia Standards (AS 2758.7, 1996) [28]. The particle size distribution of the ballast had an average particle size d_{50}=38 mm, which is similar to current Australian practices. To simulate actual field conditions, a 150 mm-thick subballast and subgrade layer, made from coarse sand and gravel mixture (unit weight of 18.5 kN/m^3), was placed at the bottom of the apparatus. The ballast was then filled above the sub-ballast and compacted in every 50 mm-thick sublayers to an actual unit weight of approximately 15.5 kN/m^3, until the final height of the ballast layer attained 300 mm. Mechanics parameters of the ballast specimen, subballast and subgrade layer tested in the laboratory is given in the Table 1.

A lateral confining pressure of σ_{xx}=10 kPa was applied in the direction parallel to sleepers to simulate low confinement given by the shoulder ballast in the field. Lateral displacement was not allowed along the direction of train passage to simulate plane strain condition, simulating a straight track where the displacement of ballast in this direction was measured very small compared to the lateral displacement parallel to the sleepers [29, 30]). The four vertical walls of the apparatus were connected with a system of ball bearings and hinges which allowed them to move horizontally with minimum resistance. Cyclic loads were applied via dynamic actuator having a maximum induced cyclic stress of σ_{yy}=420 kPa, frequency of f=15 Hz, simulating a freight train (i.e. axle load: 30 tonnes; speed: 90 km/h). All tests were conducted up to 500,000 load cycles. The detailed experimental program and analysis of these tests were presented elsewhere by Indraratna et al. [3] and they concluded that the ballast showed a significant deformation within the first 100,000 load cycles, followed by a decreased rate of settlement up to 300,000 cycles, and then kept almost constant toward the end of tests. Ballast breakage was quantified after the completion of every test by comparing the differences of ballast particle size distribution curves before and after every test, using the ballast breakage index (BBI) proposed earlier by Indraratna et al .[31]. Some of the results of these tests are re-used in this study to calibrate and validate the combined DEM-FEM model.

Table 1. Grain size characteristics of ballast and sub-ballast and subgrade

Test type	Particle shape	d_{max} (mm)	d_{10} (mm)	d_{30} (mm)	d_{50} (mm)	d_{60} (mm)	C_u	C_c
Ballast	Highly angular	53	16	28	35	39	2.4	1.3
Sub-ballast	Angular to rounded	19	0.23	0.45	0.61	0.8	3.5	1.1
Subgrade	Well graded	4.75	0.175	0.31	0.48	0.7	2.3	1.0

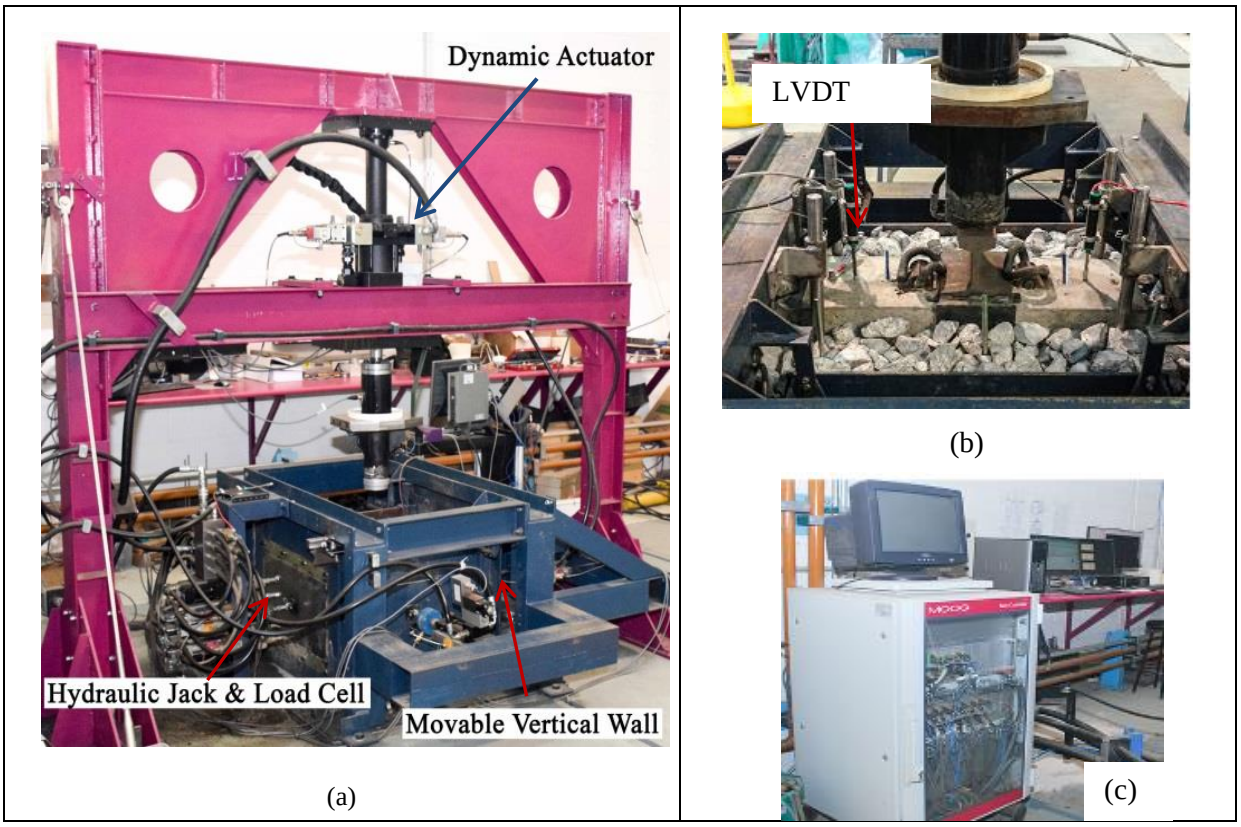

Fig.1. (a) Track Process Simulation Apparatus –TPSA; (b) Ballast assembly; (c) Data logger instrumentations

3. Coupled DEM-FEM analysis

The schematic geometric model of combined discrete-continuum approach (i.e. coupled DEM-FEM) is presented in Figure 2, where the model dimensions represent the large-scale TPSA. Given that the movement of ballast in the longitudinal direction (along with the direction of train passage) is very small due to the confinement provided by embedded sleepers, the current analysis is carried out in an equivalent plane strain condition that is usually representative of long and straight tracks. A ballast layer was modelled using the DEM - Particle Flow Code, PFC2D, whereas subgrade layer was modelled by continuum approach using the Fast Lagrangian Analysis of Continua, FLAC. The interaction between ballast layer and subballast was achieved through interface elements at the DEM and FEM boundary. Principally, the coupling between the DEM and FEM was achieved at the ballast-subgrade interface by: (i) applying the forces acting on the discrete particles as force boundary conditions to the continuum grids, and (ii) treating the continuum nodal displacements as velocity boundary conditions for the discrete elements. A mathematical framework to assist the coupled model in transferring the forces and displacements between the two domains is presented in the following sections. In the current DEM analysis, the material properties of the coupled DEM-FEM numerical model are given in Table 2.

Table 2. Micro-mechanical parameters of ballast particles and walls applied in DEM simulation

Micro-mechanical parameters	Values
Radius of particle (m)	1.8×10^{-3} - 16×10^{-3}
Inter-particle coefficient of friction	0.80
Particle normal and shear contact stiffness (N/m)	3.58×10^{8}
Normal and shear stiffness of wall (N/m)	3×10^{7}
Parallel bond normal and shear stiffness (N/m)	6.25×10^{10}
Parallel bond normal and shear strength (N/m^2)	5.78×10^{6}
Parallel bond radius multiplier	0.5
Particle unit weight (kN/m^3)	15.5

3.1 Interface elements

Interface elements were created at the boundary of ballast and subballast to assist the implementation of the coupling process where conditions of equilibrium and compatibility have to be satisfied at the interface. Assuming an interface element (segment) was defined by end-point locations, X_1, X_2; a length, L and a particle contact force, $\mathbf{F} = \mathbf{F_1} + \mathbf{F_2}$, acts at the particle centroid, X_p, as illustrated in Figure 3. The contact forces acting at the segment end points, F_1, and F_2 were described in terms of shear and normal component vectors with corresponding unit vectors, $\hat{t}$ and $\hat{n}$:

$$\mathbf{F_1} = F_{1_X}\hat{t} + F_{1_Y}\hat{n} \quad (1)$$

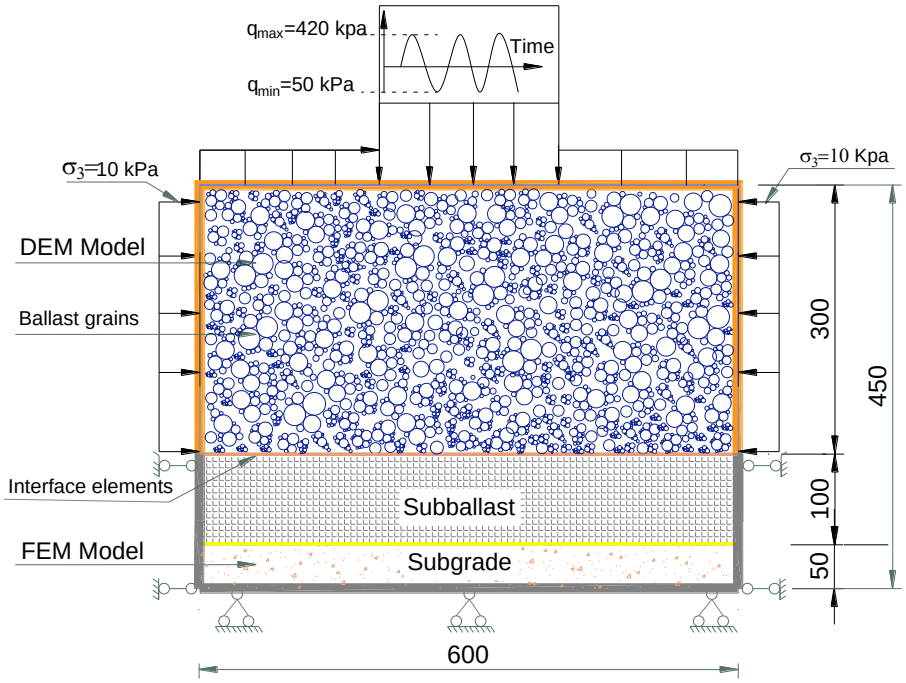

Fig. 2. Combined DEM-FEM to model TPSA for ballast (*modified after Ngo et al. [25]*)

$$\mathbf{F_2} = F_{2_X}\hat{t} + F_{2_Y}\hat{n} \tag{2}$$

The force components F_{1_X}, F_{1_Y}, F_{2_X}, and F_{2_Y} were determined by satisfying a condition that the force acting at the segment end points should produce the same moment about X_1 as the particle contact force:

$$d_1 \times \mathbf{F} = L\hat{t} \times \mathbf{F_2} = L\hat{t} \times (F_{2_X}\hat{t} + F_{2_Y}\hat{n}) \tag{3}$$

$$d_1 \times \mathbf{F} = LF_{2_X}(\hat{t} \times \hat{t}) + LF_{2_Y}(\hat{t} \times \hat{n}) \tag{4}$$

$$\text{or, } (d_{1x}\hat{t} + d_{1y}\hat{n}) \times \left(F_x\hat{t} + F_y\hat{n}\right) = LF_{2_Y}(\hat{t} \times \hat{n}) \tag{5}$$

given that: $\hat{t} \times \hat{t} = 0$; $\hat{n} \times \hat{n} = 0$; and $\hat{t} \times \hat{n} = \hat{k}$;

$$\text{results in: } (d_{1x}F_y - d_{1y}F_x)\hat{k} = LF_{2_Y}\hat{k} \text{ , or } F_{2_Y} = \frac{(d_{1x}F_y - d_{1y}F_x)}{L} \tag{6}$$

Distributing the shear components based on the nearest of X_p to each end point to obtain F_{1_X}, as given:

$$F_{1_X} = \left(\frac{|\boldsymbol{d_2}|}{|\boldsymbol{d_1}|+|\boldsymbol{d_2}|}\right)(\mathbf{F} \cdot \hat{t}) \tag{7}$$

The forces acting at the segment end points should produce the same total force as the particle reaction force: $\mathbf{F} = \mathbf{F_1} + \mathbf{F_2}$ (8)

Expressing Eq. (8) in terms of the unit-tangent vector**,** which gives two equations:

$$F_x = \left(F_{1_X} + F_{2_X}\right)t_x - \left(F_{1_Y} + F_{2_Y}\right)t_y \tag{9}$$

$$F_y = \left(F_{1_X} + F_{2_X}\right)t_y + \left(F_{1_Y} + F_{2_Y}\right)t_x \tag{10}$$

Re-arranging Eqs. (9) and (10), results in:

$$F_{1_Y} = \left[\left(F_y - F_{2_Y}t_x - F_{1_X}t_y\right)t_x + \left(-F_x - F_{2_Y}t_y + F_{1_X}t_x\right)t_y\right]/2 \tag{11}$$

$$F_{2_X} = \begin{cases} \frac{F_x + (F_{1_Y} + F_{2_Y})t_y - F_{1_X}t_x}{t_x} \\ \frac{F_y - (F_{1_Y} + F_{2_Y})t_x - F_{1_X}t_y}{t_y} \end{cases}, \text{ or} \tag{12}$$

When the above equations are applied, it is assured that the segment forces acting on the FEM model (F_{1_X}, F_{1_Y}, F_{2_X}, and F_{2_Y}) produced the same total force and moment as particle contact forces acting on the DEM model. Thus, the DEM and FEM model along the interface boundary will both experience the same overall loading condition. Subroutines written in the FISH language were developed by the authors to employ all the aforementioned equations to implement a fully coupled DEM-FEM analysis. It is also noted that the forces acting on the discrete particles will not totally apply on the subballast due to losses of energy or forces at their interfaces. In the current DEM analysis, the energy losses and force losses are presumably small and therefore they are negligible.

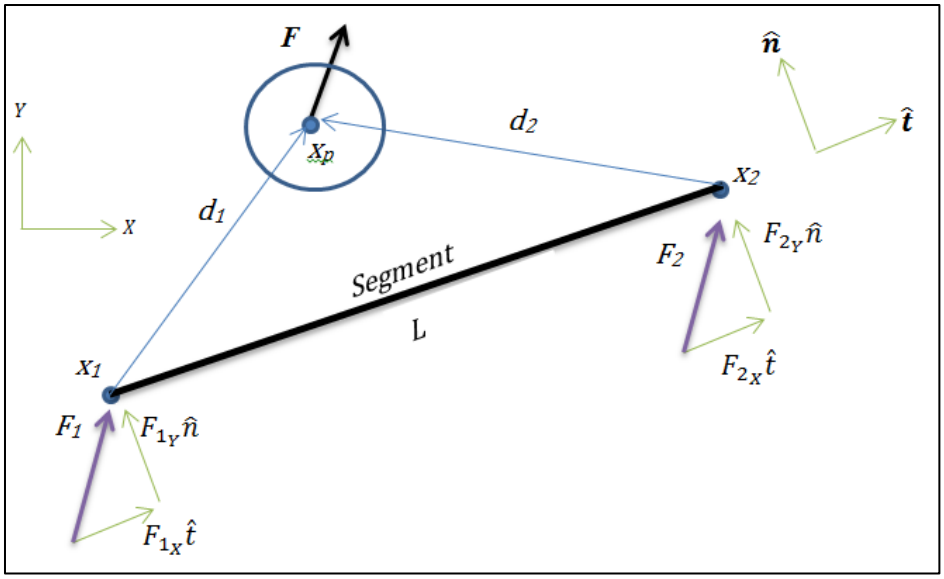

Fig. 3. Distributing particle contact forces to segment end points (*modified after Ngo et al. [25]*)

4. Results and discussion

4.1. Load-deformation analysis

Figure 4 illustrates the applied cyclic stress versus accumulated axial strain obtained from the coupled DEM-FEM analysis at varying load cycles. It is noted that the plastic deformation of the ballast (i.e. basalt rock) is observed in the DEM analysis. The accumulated axial strain results are shown in Figure 4 is for ballast layer only, excluding any strains for subballast and subgrade layer. It is seen that the predicted axial strains increase remarkably within the first 1000 load cycles (i.e. up to around 3% axial strain), followed by gradually increasing axial strains within 5,000 cycles, and then remained relatively stable to the end (10,000 cycles). These results are in good agreement with those measured in the laboratory [3]. Indeed, the area confines by the cyclic (hysteresis) loops becomes increasingly smaller as the number of cycles increases, indicating that the ballast specimen through cyclic densification begins to respond more elastically with time. The hysteresis loops are also very similar to those obtained in laboratory experiments and simulations. The predicted axial and lateral strains are compared with those measured by Indraratna et al. [3], as shown in Figure 5. It is noted that the axial strains were computed excluding the deformations of capping and subgrade layers. In this context, the limited thickness of sand layer used in the laboratory is considered as a reasonable approximation of the subgrade layer in the current analysis. Generally, the predicted strains agree well with experimental data, showing that most strains have taken place after the first 100 cycles, and beyond which the increments of permanent deformation considerably decrease. This indicates that the ballast sample undergoes considerable rearrangement and densification during initial load cycles, but after attaining a threshold compression, any subsequent loading would resist further deformation and promote particles crushing [32, 33]. This finding is in agreement with results presented by Lobo-Guerrero and Vallejo [34] where they observed that the ballast deformation considerably increased when the particle breakage was considered analysis. The coupled analysis shows a noticeable discrepancy in the strain curves, i.e., markedly increase in strain at load cycles of N=5000-8000 compared with the experimental data. This difference may be attributed to excessive particle degradation (i.e. bond breakage) that could not be accurately captured in the coupled model and the rigidity of the loading plate. Indeed, owing to the breakage of contact bonds, it would increase the compression of the ballast assembly, and would also be accompanied by an increase in lateral strain.

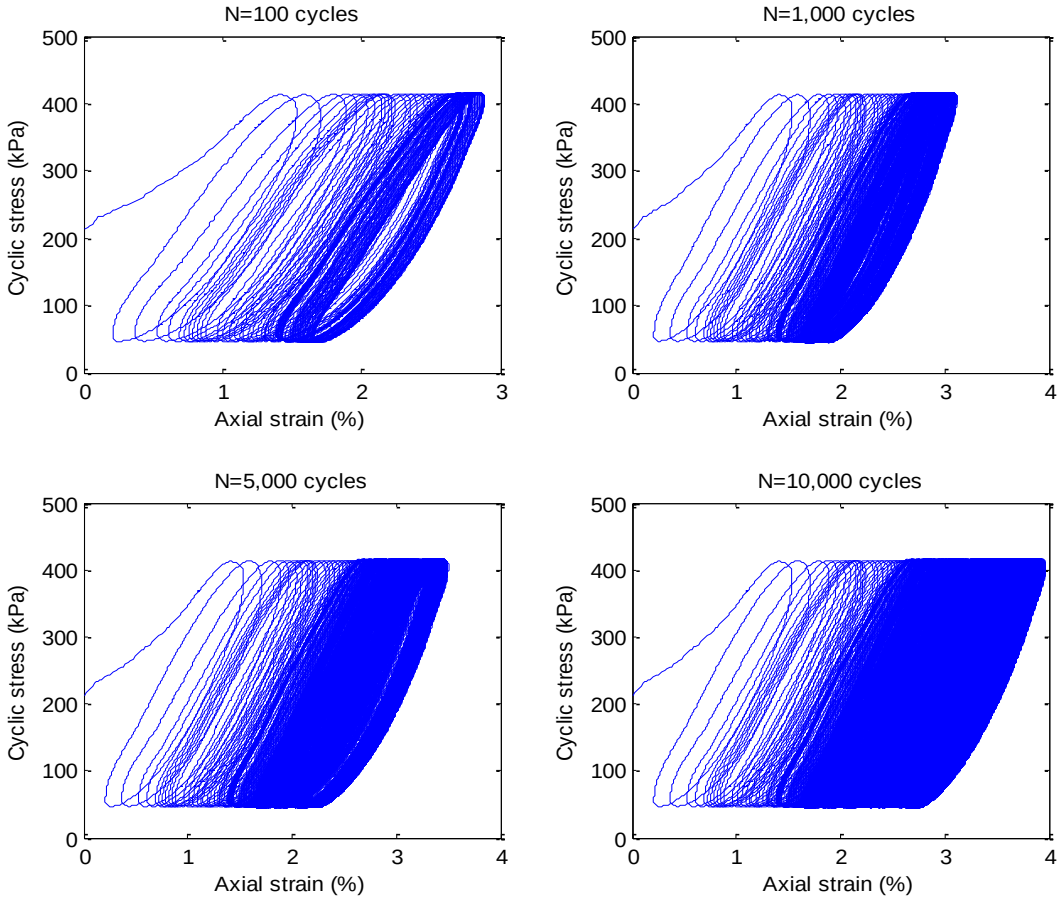

Fig. 4. Applied cyclic stress versus axial strain at varying number of load cycles.

4.2. Contact forces and stress analysis

The applied cyclic loads transmit to the discrete ballast particles in a form of contact force-chains where the pattern of force-fabric varies with packing structure and substantial controls the deformation and strength behaviour of the ballast assembly [9, 30]. Figure 6 presents the inter-particle forces of the ballast assembly together with vertical stress contours at different load cycles of *N*=10, 1000 and N=5000 cycles. Each contact force is represented at the contact point by a black line oriented in the direction of the contact force and with a thickness proportional to the intensity of the force. It is seen that the majority of contact forces are distributing in a vertical direction (i.e. major principal stress direction) which is transmitting the applied cyclic loads downwards through the ballast assembly. Upon repeated loading, there is a concentration of large contact forces occurring beneath the loading plate (i.e. sleeper), and around wall edges, while a significant part of the applied load is still vertically transmitted to the underneath subgrade (Figure 6b, 6c). It is also noted that the force distribution in the DEM region shows heterogeneous, where the maximum contact forces substantially vary with load cycles. These forces create the deformation of the assembly (i.e., vertical and lateral displacements) and the breakage of contact bonds (i.e., particle breakage).The compressive stress (σ_{yy}) in the subgrade is greater mainly around the interface area that is directly in contact with the ballast aggregates, whereby it is predicted to considerably decrease with depth (Figure 6).

4.3. Particle breakage

In the current coupled DEM-FEM analysis, the disconnection of contact bonds within a cluster of ballast are considered to represent ballast breakage. It is noted that the particle shape and size of realistic ballast grains are simulated by clusters of bonded circular particles; and the degradation of bonds within a cluster was possibly considered to represent ballast breakage. Once the applied contact forces exceed the contact bonds, the breakage of contact bonds occurs. Figure 7 shows the snapshots of the evolution of bond breakage at varying number of cyclic loads under a given load frequency of f=15 Hz. The number and locations of bond breakages at different stages of cyclic loading, varying from 100 cycles to 10,000 cycles are presented in Figures 7a-f. It is seen that, within the first 100 cycles, the majority of the bond breakage occurs right underneath the loading plate due to induced high contact forces, as shown in the Figure 7a. With an increase in cyclic loads there is an increase in the bond breakage (Figures 7b-f) and the re-arrangement of broken particles (i.e. particles get compacted and ceased from further breaking), which results in solid and more uniform contact force distributions in the major principal stress direction as shown in Figures 6b-c. It is seen that the evolution of broken bonds is very similar to the increased ballast breakage observed from the laboratory data [3]. This phenomenon clearly explains that the formation of contact force distributions in the ballast assembly during cyclic loading is a dynamic process, significantly influenced by the breakage of the particles. Figure 7g illustrates typical locations and re-arrangement of broken particles during cyclic loading where bonds are broken and the corresponding particles are separating each other, representing particle breakage.

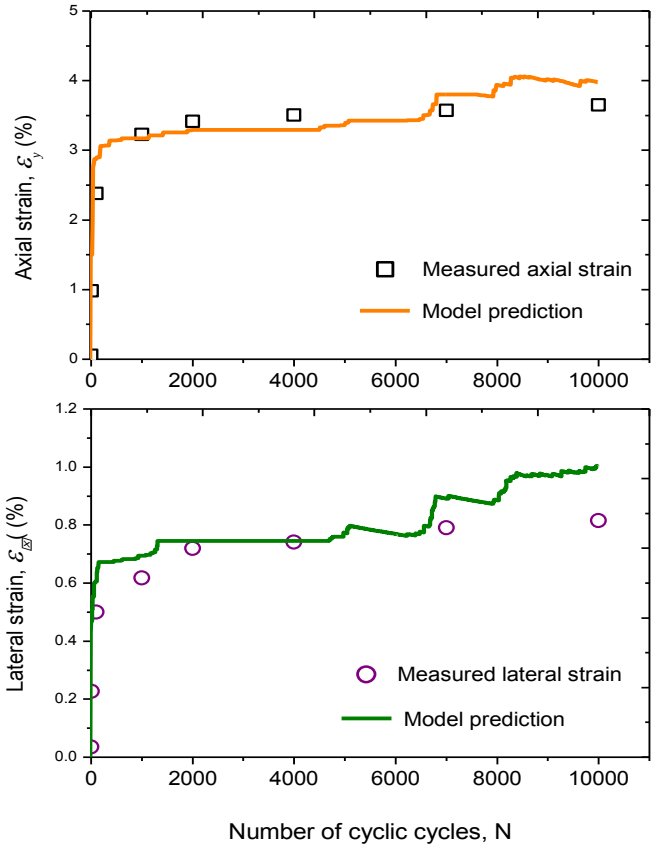

Fig. 5. Comparisons of axial strain and lateral strains obtained from coupled DEM-FEM simulations with data measured experimentally (*modified after Ngo et al. [25]*)

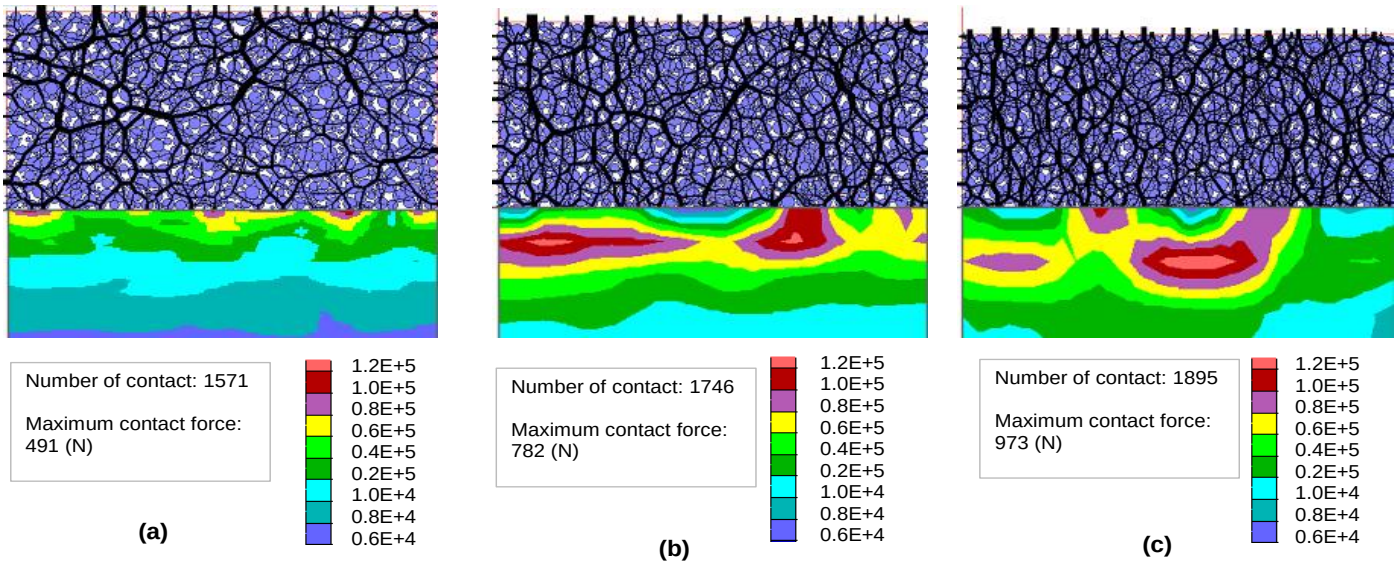

Fig. 6. Contact forces and rertical stress contour (σ_{yy}) developed in discrete and continuum media at varying load cycles; (a) 10 cycles; (b) 1000 cycle; and (c) 5000 cycles

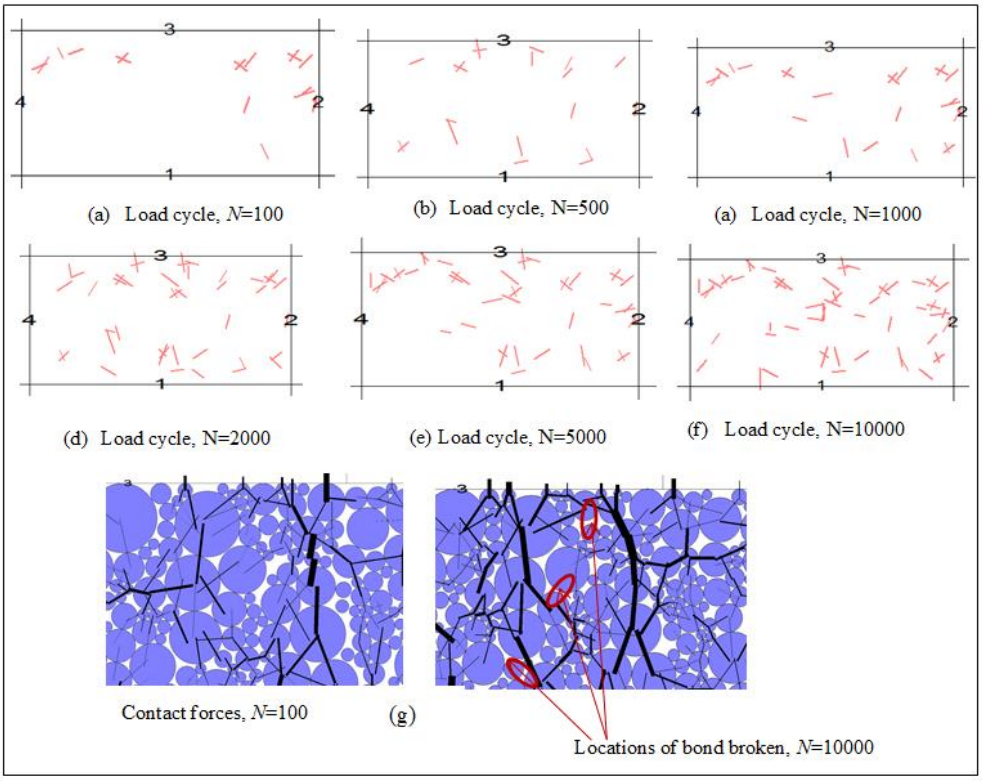

Fig. 7. Snapshots of bond breakage at varying load cycles: N=100; (b) N=500; (c) N=1000; (d) N=2000; (e) N=5000; (f) N=10000

5. Applying the coupled DEM-FEM analysis for Singleton track

The proposed DEM-FEM model was used to predict load-deformation the settlement behaviour of an actual track subjected to cyclic loading where a half track modelling of the Singleton track (located about

200 km from Sydney, NSW, Australia) was considered [25]. Field data measured at Singleton track carried out by Indraratna et al. [35] were used to compare with those obtained from the DEM-FEM analysis. The field trial was carried out on a section of instrumented track located near Singleton, NSW where two types subgrade of relatively soft general fill and hard rock (i.e. Section A and Section C) were investigated. The track substructure consisted of a 300 mm ballast placed over a 150 mm thick capping and a structure fill with the thickness varying from 500 mm to 900 mm was placed below. Comparisons of the settlement response, S_v of ballast for two types of subgrades obtained from the combined model and those measured in the field is presented in Figure 8. It is noted that the boundary conditions, and applied cyclic loads were modelled similarly to those carried out in the field (i.e. mean cyclic stress of 235 kPa; frequency of 15 Hz) to simulate a freight train having axle load between 25 and 30 tons travelling at about 80 km/h. It is evident that the model predicts the vertical deformations of ballast quite well in relation to the observed deformation measuring using settlement pegs in the field, where only a slight deviation from the measured data was found. Subjected to 10,000 load cycles, the measured value of S_v for hard subgrade of 6.07 mm compares well with the predicted values of 6.71 mm. A slight increase in settlement predicted for the case of soft subgrade (S_v =10.21 mm) compared to a value of S_v = 8.72 mm measured in the field, and this may be attributed to some discrepancies of the boundary conditions between the field and the coupled model where a plane strain condition was considered in the current analysis.

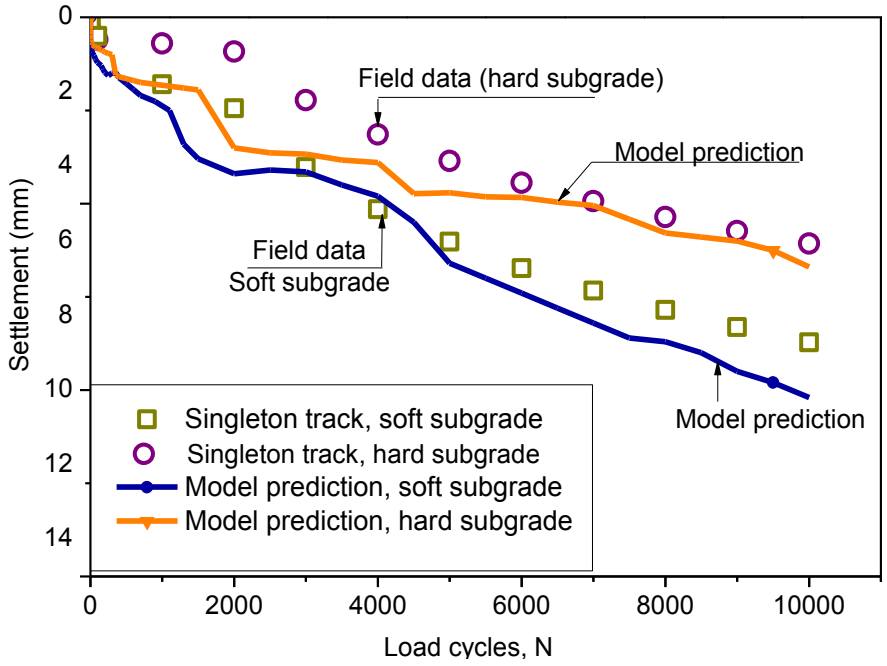

Fig. 8. Comparisons of settlements between the model and field data (*after Ngo et al. [25]*).

6. Conclusions

Large-scale track process simulation apparatus (TPSA) tests were carried out to study the load-deformation responses of rail ballast under cyclic loading. Experimental results indicated that the ballast exhibited a significant axial strain in initial load cycles, followed by gradually increasing deformation and then remained relatively unchanged toward the end. A combined discrete-continuum model was introduced to study load-deformation responses of ballast in a plane strain condition where the ballast aggregates were modelled by the discrete element method and the subgrade was modelled by finite continuum approach. Irregularly-shaped ballast particles were simulated in DEM by connecting of specified numbers of circular balls together to represent appropriate angularity and sizes. Subgrade and

subballast were modelled using continuum method, having a total thickness of 150 mm to simulate capping formation in the field.

Results of the axial strains obtained from the coupled DEM-FEM model were comparable with experimental data, indicating that the proposed model could capture the load–displacement behaviour of the ballast subjected to cyclic loading. Evolutions of contact force distributions and stress contours induced in the ballast at varying stages of cyclic loading were analysed and it confirmed that the stresses distributed non-uniformly across the ballast assembly where the maximum stresses occurring beneath the sleeper resulting in greater number of broken bond observed. The proposed coupling DEM-FEM model was also used to predict the load-deformation response of the instrumented Singleton track where two types of subgrade (e.g. relatively soft and hard subgrade) were considered. The predicted settlement results were comparable with the measured field data showing that the proposed coupling model can be used to predict the load-deformation behaviour of ballasted tracks.

Acknowledgements

The Authors would like to acknowledge the Rail Manufacturing CRC, Australasian Centre for Rail Innovation (ACRI) Limited, and Tyre Stewardship Australia Limited (TSA) for providing the financial support needed to undertake this research (Project R2.5.1). The Authors are grateful to Mr. Alan Grant, Mr. Cameron Neilson, Mr Duncan Best and Mr. Ritchie McLean for their assistance in the laboratory and field works. Field works (Singleton) carried out by Dr. Nimbalkar is also greatly appreciated.

References

[1] Selig, E.T. and Waters, J.M. Track geotechnology and substructure management. 1994: Thomas Telford, London.
[2] Indraratna, B., Ngo, NT, and Rujikiatkamjorn, C. Behavior of geogrid-reinforced ballast under various levels of fouling. Geotextiles and Geomembranes, 2011. 29(3): 313-322.
[3] Indraratna, B., Ngo, NT, and Rujikiatkamjorn, C. Deformation of coal fouled ballast stabilized with geogrid under cyclic load. Journal of Geotechnical and Geoenvironmental Engineering, 2013. 139(8): 1275-1289.
[4] Tutumluer, E., Huang, H. and Bian, X. Geogrid-aggregate interlock mechanism investigated through aggregate imaging-based discrete element modeling approach. International Journal of Geomechanics, 2012. 12(4): 391-398.
[5] Suiker, A.S.J., Selig, E.T. and Frenkel, R. Static and cyclic triaxial testing of ballast and subballast. Journal of Geotechnical and Geoenvironmental Engineering, ASCE 2005. 131(6): 771–782.
[6] Rujikiatkamjorn, C., Indraratna, B., Ngo, NT, and Coop, M. A laboratory study of railway ballast behaviour under various fouling degree. The 5th Asian Regional Conference on Geosynthetics, 2012: 507-514.
[7] McDowell, G.R., Lim, W.L., Collop, A.C., Armitage, R. and N.H. Thom. Comparison of ballast index tests for railway trackbeds. Geotechnical Engineering, 2008. 157(3): 151–161.
[8] Biabani, M.M., Ngo, NT, and Indraratna, B. Performance evaluation of railway subballast stabilised with geocell based on pull-out testing. Geotextiles and Geomembranes, 2016. 44(4): 579-591.
[9] Indraratna, B., Nimbalkar, S.S., Ngo, NT, and Neville, T. Performance improvement of rail track substructure using artificial inclusions – Experimental and numerical studies. Transportation Geotechnics, 2016. 8: 69-85.
[10] Biabani, M.M., Indraratna, B., and Ngo, NT. Modelling of geocell-reinforced subballast subjected to cyclic loading. Geotextiles and Geomembranes, 2016. 44(4): 489-503.
[11] Salim, W. Deformation and degradation aspects of ballast and constitutive modeling under cyclic loading. 2004, PhD Thesis, University of Wollongong, Australia.
[12] Bolton, M.D., Nakata, Y. and Cheng, Y.P. Micro- and macro-mechanical behaviour of DEM crushable materials. Geotechnique, 2008. 58(6): 471–480.
[13] McDowell, G.R. and Harireche, O. Discrete element modelling of soil particle fracture. Geotechnique, 2002. 52(2): 131-135.

[14] Cundall, P.A., and Strack, O.D.L. A discrete numerical model for granular assemblies. Geotechnique, 1979. 29(1): 47-65.
[15] Cui, L. and O'Sullivan, C. Exploring the macro- and micro-scale response of an idealised granular material in the direct shear apparatus. Geotechnique, 2006. 56(7): 455-468.
[16] Cheng, Y.P., Bolton, M.D and Nakata, Y. Crushing and plastic deformation of soils simulated using DEM. Geotechnique, 2004. 54(2): 131-141.
[17] Ngo, N.T., Indraratna, B., Rujikiatkamjorn, C., and Biabani, M. Experimental and discrete element modeling of geocell-stabilised subballast subjected to cyclic loading. Journal of Geotechnical and Geoenvironmental Engineering, 2016. 142(4): 04015100.
[18] Ngo, N.T., Indraratna, B., and Rujikiatkamjorn, C. DEM simulation of the behaviour of geogrid tabilised ballast fouled with coal. Computers and Geotechnics, 2014. 55: 224-231.
[19] Lobo-Guerrero, S. and Vallejo, L.E. Discrete element method evaluation of granular crushing under direct shear test condition. Journal of Geotechnical and Geoenvironmental Engineering, 2005. 131(10): 1295-1300.
[20] Oda, M. and Iwashita, K. Mechanics of granular materials: An introduction. 1999: Rotterdam: A. A. Balkema.
[21] Ngo, N.T., Indraratna, B, and Rujikiatkamjorn, C. Modelling geogrid-reinforced railway ballast using the discrete element method. Transportation Geotechnics, 2016. 8(2016): p. 86-102.
[22] McDowell, G.R., Harireche, O., Konietzky, H., Brown, S.F., and Thom, N.H. Discrete element modelling of geogrid-reinforced aggregates. Proceedings of the ICE - Geotechnical Engineering 2006. 159(1): 35-48.
[23] Bhandari, A. and Han, J. Investigation of geotextile-soil interaction under a cyclic vertical load using the discrete element method. Geotextiles and Geomembranes, 2010. 28(1): 33-43.
[24] Zhang, X., Zhao, C., and Zhai, W. Dynamic Behavior Analysis of High-Speed Railway Ballast under Moving Vehicle Loads Using Discrete Element Method. International Journal of Geomechanics, 2016: 04016157.
[25] Ngo, N.T., Indraratna, B., and Rujikiatkamjorn, C. Stabilisation of track substructure with geo-inclusions – experimental evidence and DEM simulation. International Journal of Rail Transportation, 2017. DOI: http://dx.doi.org/10.1080/23248378.2017.1279085.
[26] Lu, M. and G.R. McDowell. Discrete element modelling of railway ballast under monotonic and cyclic triaxial loading. Geotechnique, 2010. 60(6): 459-467.
[27] Indraratna, B., W. Salim, and C. Rujikiatkamjorn. Advanced Rail Geotechnology - Ballasted Track. 2011a: CRC Press, Taylor & Francis Group, London, UK
[28] AS 2758.7, A. Aggregates and rock for engineering purposes, Part 7. Railway Ballast. Standard Australia, 1996. NSW, Australia.
[29] Indraratna, B., S. Nimbalkar, D. Christie, C. Rujikiatkamjorn, and J.S. Vinod. Field assessment of the performance of a ballasted rail track with and without geosynthetics. Journal of Geotechnical and Geoenvironmental Engineering, ASCE, 2010b. 136(7): 907–917.
[30] Ngo, N.T. and Indraratna, B. Improved performance of rail track substructure using synthetic inclusions: Experimental and numerical investigations. International Journal of Geosynthetics and Ground Engineering, 2016. 2(3): 1-16.
[31] Indraratna, B., J. Lackenby, and D. Christie. Effect of confining pressure on the degradation of ballast under cyclic loading Geotechnique, 2005. 55(4): 325–328.
[32] Ngo, N.T., Indraratna, B., and C. Rujikiatkamjorn. Micromechanics-based investigation of fouled ballast using large-scale triaxial tests and discrete element modeling. Journal of Geotechnical and Geoenvironmental Engineering, 2017. 134(2): 04016089.
[33] Biabani, M.M. and Indraratna, B. An evaluation of the interface behaviour of rail subballast stabilised with geogrids and geomembranes. Geotextiles and Geomembranes, 2015. 43(3): 240-249.
[34] Lobo-Guerrero, S. and L.E. Vallejo, Discrete element method analysis of railtrack ballast degradation during cyclic loading. Granular Matter, 2006. 8(3-4): 195-204.
[35] Indraratna, B., Nimbalkar, S. and T. Neville. Performance assessment of reinforced ballasted rail track. Proceedings of the ICE - Ground Improvement, 2014. 167: 24-34.